# Microfabricated Cylindrical Multielectrodes for Neural Stimulation

Sean Snow, *Member, IEEE*, Stephen C. Jacobsen, *Member, IEEE*, David L. Wells, and Kenneth W. Horch*, *Member, IEEE*

***Abstract*—The effects of spinal cord injuries are likely to be ameliorated with the help of functional electrical stimulation of the spinal cord, a technique that may benefit from a new style of electrode: the cylindrical multielectrode. This paper describes the specifications for, fabrication techniques for, and *in vitro* evaluation of cylindrical multielectrodes. Four tip shapes were tested to determine which shape required the lowest peak force and would, therefore, be expected to minimize dimpling during implantation. The impedance of the electrode interface was monitored for changes due to insertion as well as repetitive delivery of current pulses. The charge delivery capacity was determined by testing with safe ($\leq 0.6$ mC/cm$^2$) and damaging levels ($\geq 0.8$ mC/cm$^2$) of charge density. The results of these tests suggest that this electrode design could be used to stimulate neurons in the ventral horn of the spinal cord.**

***Index Terms*—Depth electrodes, impedance testing, microelectromechanical systems (MEMS), microstimulation, neural prosthesis.**

## I. Introduction

In the pursuit of functional rehabilitation of paralyzed muscles by electrical means, motor point and peripheral nerve stimulation have generated many successes [1]–[3]. A major problem with using stimulation at the periphery is the mismatch of mechanical properties between the biological tissue and the electrode materials, which is aggravated by the relative movement between the target and surrounding tissues. One way of reducing this problem is to implant neural interfaces in areas that experience less movement relative to overlying tissues, such as the central nervous system.

Intraspinal stimulation has been shown to provide graded, muscle-selective recruitment of hindlimb muscles with long-term stability [4]. In this prior research, electrodes were constructed from stainless-steel wires which were bent and inserted into the lumbro-sacral spinal cord. This type of wire electrode yields a single stimulation site within the ventral horn of the spinal cord at a depth that is decided prior to the surgery. Intraspinal stimulation would benefit from an electrode that could be implanted into the spinal cord and provide simultaneous access to several levels of the motor pool.

By creating an electrode with a circular cross section instead of a rectangular cross section, tissue in the nervous system should better tolerate the electrode's presence compared to traditional, planar fabricated electrodes with sharp corners. The rectangular cross section Michigan array [5] has recently been modified to a semi-circular cross section for improved insertability while "minimizing tissue damage" [6]. However, this approach limits electrode site and circuit trace production to less than half of the substrate's outer surface. In contrast, cylindrical microfabrication allows feature creation on the substrate's entire surface. We suggest, then, that the best design for intraspinal stimulation electrodes may be cylindrical multielectrodes capable of insertion into and stimulation of the spinal cord.

For long-term implantation in an awake and freely-moving animal, the electrode should be at least 4 mm long to reach the ventral horn of the spinal cord, have a connector region (extending above the dorsal surface of the cord) less than 250 $\mu$m long, and be less than 100 $\mu$m in diameter to minimize tissue displacement. In the past, groups have built cylindrical multielectrodes that are not suitable for chronic implantation due to overly large diameters (1000 $\mu$m) or lengths (31 mm) [7], [8]. The electrode described in this paper can be configured for up to ten stimulation sites at arbitrary spacing along a cylinder. For this study, specific parameters were chosen to best match the environment of the motor pools in the ventral horn of the feline lumbro-sacral spinal cord [9]. The electrode specifications were set at four stimulation sites, spaced 400 $\mu$m apart and located 2.4–4.0 mm deep from the dorsal surface of the spinal cord. By using microfabrication processes developed specifically for cylindrical substrates [10], [11] (Snow, unpublished observations), electrodes with these specifications were built on cylinders with a diameter of 85 $\mu$m.

In addition to size and mechanical specifications, the electrodes were required to deliver sufficient charge for intraspinal stimulation to elicit muscle contraction without degradation of the electrodes, as determined by either large impedance changes, loss of electrode metal, or disruption of the insulation layer. Each stimulation site was required to safely pass 0.4 mC/cm$^2$ as this limit was found to be safe for both platinum and iridium [12], [13] yet sufficient to excite neural tissue in the spinal cord [14].

Manuscript received October 4, 2004; revised April 17, 2005. This work was supported in part by the National Institutes of Health through the National Institute of Neurological Disorders and Stroke (NINDS). *Asterisk indicates corresponding author.*

S. Snow, was with the Department of Bioengineering, University of Utah, Salt Lake City, UT 84112 USA (e-mail: s.snow@m.cc.utah.edu).

S. C. Jacobsen is with the Sarcos Research Corporation, Salt Lake City, UT 84108 USA (e-mail: jacobsen@ced.utah.edu).

D. L. Wells is with the Bloorview MacMillan Children's Centre, Toronto, ON M4G 1R8, Canada (e-mail: dwells@bloorviewmacmillan.on.ca).

*K. W. Horch is with the Department of Bioengineering, 50 S. Central Campus Dr., University of Utah, Salt Lake City, UT 84112 USA (e-mail: k.horch@utah.edu).

Digital Object Identifier 10.1109/TBME.2005.862552

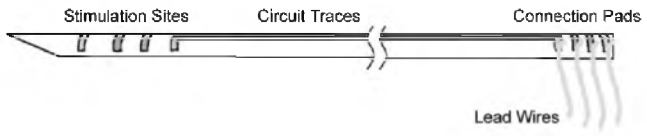


Fig. 1. Electrode design. Circuit traces run down the shaft to link each connection pad to one stimulation site. Lead wires are bonded to the connection pads. The electrode components are not to scale.

## II. Methods

Fig. 1 shows the target electrode design with the stimulation sites, circuit traces, and connection pads microfabricated on a cylinder. Gold lead wires connect the connection pads to external electronics.

### A. Electrode Fabrication

*1) Fiber Preparation:* Standard optical fiber (FIP 050 070 085, PolyMicro Technologies) was chosen as the substrate for the electrodes because of its mechanical properties. The fiber is robust enough to withstand repeated bending to ninety degrees and the rigid quartz core allows precision tip sharpening and stable fiber positioning during photolithography.

A 7-mm-long piece of 85-$\mu$m-diameter fiber was attached to a silicon wafer and one end was bevelled using a dicing saw (DAD-2H/6, Disco Abrasive Systems) cutting at 300 $\mu$m/s to form a sharpened tip. The polyimide coating on the fiber was stripped from the tip to prevent it from catching on tissue during insertion by placing the fiber tip next to a white-hot platinum filament. This left a 40–80 $\mu$m zone of tapered polyimide.

*2) Metallization:* After preparing the tip of the fiber, the fiber was ultrasonically cleaned in acetone, surfactant (Micro-90, Cole Parmer), and deionized water and then baked in a convection oven at 80 °C for 5 min to remove any water. The fiber was then loaded into a rotary-sputtering fixture, placed in the sputtering system chamber (PVD300, Unifilm Technologies), and vacuumed to less than 2.7 mPa. The adhesion layer, 500 Å of chrome, was sputtered onto the fiber followed by 15 000 Å of gold as the electrically conductive layer.

*3) Photolithography:* The metallized fiber was dip coated with 5 $\mu$m of positive photoresist (HD-8000, HD Microsystems) by pulling it out of a pool of photoresist at a rate of 14 mm/min. The coated fiber was prebaked at 120 °C for 100 s and was then prepared for exposure by loading it into the cylindrical lithography system [10], [11], [15]. A He-Cd laser was used to create 10 $\mu$m linewidths. Development of the exposed photoresist required 55 s of immersion in tetramethyl ammonium hydroxide (MF-321, Shipley Company). This left photoresist on the areas designated to be bonding pads, electrical traces, and stimulation sites ($\sim$ 140 $\mu$m wide by $\sim$ 70 $\mu$m long). The gold layer was then removed from the uncoated areas by wet etching for 85 s in tri-iodide etchant (400 g KI, 200 g $I_2$, 1000 ml $H_2O$), resulting in less than 2 $\mu$m of undercut. The chrome layer was etched away in perchloric acid until the circuit traces were electrically isolated. A photoresist stripper (Microposit 1165, Shipley Company) was used to clean away the remaining photoresist.

The fiber was recoated with HD-8000 photoresist, and a new pattern was exposed onto the surface and developed away. This uncovered the bonding pads and stimulation sites while insulating the conductive traces and the remainder of the fiber. HD-8000 was selected because it served both as a photoresist and as an insulator. The polyimide components of this resist were fully polymerized by curing the fiber at 350 °C for 30 min. After curing, the polymer was capable of withstanding immersion in acetone as well as any mechanical shearing forces.

*4) Connections:* Once the fiber had the metal and insulation layers complete, connections were made to gold lead wires by wire bonding. The wire bonding process was started by gluing the fiber onto a microscope slide with photoresist. Using the dicing saw system, the back end of the fiber (opposite of the tip) was cut outside of the bonding region, resulting in a final fiber length of 4.4 mm. Four, 25-$\mu$m-diameter, insulated gold wires (TC gold Type 1 H-poly red, California Fine Wire) were routed from an external connector across the bonding pads of the fiber and taped down to the microscope slide to maintain their position over the bonding pad. Bonding was achieved using a wire bonder (Mech-El 909Z, MEI) set to 55 g of weight at the tip with maximum ultrasonic power for 500 ms. Wire bonds were mechanically stabilized by a biocompatible thixotropic epoxy (FDA-2T, Tra-Con Adhesives) applied over the bonds. The connector/lead wire/fiber system was then immersed in acetone to dissolve the gluing layer of photoresist from under the electrode. After the wired electrode was released from the slide, the backside of the wire bond region was protected by a second coat of epoxy. In order to seal any possible cracks at the interface of the two epoxy coats, three coats of silicone conformal coating (422A, M.G. Chemicals) were applied to the bond region and cured in compliance to the manufacturer's schedule.

*5) Electrodeposition:* A gold surface is not preferred for an electrode interface material and, therefore, requires electroplating with either platinum or iridium. This electroplating process for the two different materials varied only in solution chemistry and deposition times. Platinum black was plated using 3% platinic chloride [16] in deionized water whereas iridium was plated using 14% hydrogen hexachloroiridate(IV) hydrate in deionized water. All four stimulation sites were submerged within the electroplating solution and 60-Hz ac current was individually passed through each stimulation site [17]. For platinum, the current was ramped via computer control from zero to 300 $\mu$A (RMS) over a 90-s period and held at 300 $\mu$A (giving a current density of 4.2 A/cm$^2$) for 40 s. Since iridium plated more slowly, the current was ramped via computer control from zero to 300 $\mu$A over a 200-s period and held at 300 $\mu$A for 200 s. No hydrolysis was observed during the plating.

After electrodeposition, the fabrication process was complete and the electrodes were ready for benchtop testing.

### B. In Vitro Testing

*In vitro* testing included investigations of tip shape, insertion effects on impedance, charge delivery capacity, and impedance stability.

*1) Tip Shape:* The shape of the electrode tip is important in minimizing damage to neural tissue during insertion. Four different shapes, referred to as blunt, slant, chisel, and hypo (Fig. 2), were tested to determine which tip would result in the

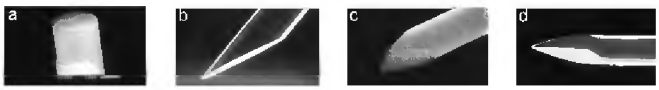


Fig. 2. Four tip styles tested for insertion forces: (a) blunt, (b) slant, (c) chisel, and (d) hypo. All fibers were 70 $\mu$m in diameter once the 7.5-$\mu$m-thick polyimide coating was ablated.

lowest insertion force. The blunt style was the easiest shape to produce and the slant style was the easiest taper to cut. The chisel style was an analogue to Edell's best-shaped silicon microshafts for cerebral cortex [18], and the hypo style was roughly fashioned after hypodermic needles. Four fibers of each style were made using the dicing saw. The chisel and hypo styles required multiple cuts. The resulting tip angles for the blunt, chisel, slant, and hypo tip shapes were approximately 180°, 40°, 20°, and 20°, respectively.

Given concerns about appropriate use of animals in research and limitations on the availability of consistent, fresh animal cadavers, testing the insertion forces required simulated neural tissue. Two layers of 20-$\mu$m-thick Saran Wrap® over tofu were used for this purpose as this has been identified as the preferred substitute by the lab for which these electrodes were fabricated (Mushahwar, personal communication).

The sharpened fibers were photographed, loaded into handling collets, and attached to a 9.8 N force transducer (Sensotec) driven by a 5-V power supply. Fiber tips were forced into simulated neural tissue while the transducer output signal was sampled at 1 kHz to determine peak insertion force. Each fiber was inserted 6 times into a new region of the material resulting in six force measurements for each fiber. Each of the 16 fibers was tested in pseudorandom order. The tips were rephotographed at the end of the testing to compare any structural changes in the tips.

*2) Insertion Effects on Impedance:* When a platinized stimulation site is inserted through a material, the interface experiences a scrubbing action that increases the interfacial impedance [16]. With this in mind, the multielectrodes were tested to determine the effect of insertion on impedance. More test insertions were used on each electrode than would be expected for surgical implantation.

Based on the results from the tests of the effects of tip shape, the slant tip style was used for the remaining tests. Three slant tip fibers containing 12 platinum-coated stimulation sites were tested to determine the effect of insertion through simulated neural tissue on the interfacial impedances. A 1 kHz, sinusoidal, 4 $\mu$A peak-to-peak current was passed through electrodes that were submerged in 37 °C phosphate-buffered saline (PBS). The voltage across each stimulation site was sampled at 60 kHz for 0.5 s and compared to the voltages across four calibration resistors to determine the impedance of the sites. Baseline impedances were established by five measurements in PBS, with air drying between each measurement. This drying step was included to help isolate the effect of drying from the effect of insertion. After the fifth measurement, the electrodes were inserted ten times into the simulated neural tissue. Locations were marked to avoid any penetrations into preexisting punctures. The impedances were then measured five more times in PBS, with air drying between each measurement. The experiment was repeated for iridium-coated sites.

*3) Charge Delivery Capacity:* Previous studies have established stimulation limits (charge density) which, if exceeded, can increase the impedance of the stimulation site and eventually destroy the electrode [19]. Since activated iridium films have five times greater charge delivery capacity than platinum films [13], testing of charge delivery capacity utilized only iridium plating. These stimulation sites were tested to determine the stimulation limit at which impedance doubled from initial measurements to post-testing measurements.

To do this, 19 stimulation sites from eight electrodes were photographed in color using a compound microscope at 500 × before testing. They were then immersed in heated PBS and given charge-balanced, 200 $\mu$s long, 50 $\mu$A cathodic-first at 50-Hz pulse trains, on for 1 s and off for 1 s for 1 h. Given the stimulation area of 0.0001 $\mathrm{cm}^2$, each current pulse delivered a charge per unit area of 0.1 $\mathrm{mC/cm}^2$. After the initial measurement of the 19 sites were complete, three of the stimulation sites were subjected to test charges of 0.4 $\mathrm{mC/cm}^2$, six of them were subjected to 0.6 $\mathrm{mC/cm}^2$ pulses, seven were subjected to 0.8 $\mathrm{mC/cm}^2$ pulses, and three were subjected to 1.6 $\mathrm{mC/cm}^2$ pulses. Throughout both the initial measurements and test measurements, impedances were measured every 15 min. Each stimulation site was photographed at the end of the test and compared to pretesting micrographs to evaluate any changes in film condition.

*4) Impedance Stability:* Ten platinum-plated stimulation sites were placed in heated PBS and stimulated once every 2 s with 1-s duration, 50-Hz pulse trains consisting of charge-balanced, 200 $\mu$s long, 100 $\mu$A pulses. Stimulation was on for 16 h per day followed by an 8-h quiescent period over a 12–day period, resulting in over 17 million stimulations per site. Interfacial impedance was measured every 10 min. Deionized water was added to the heated bath to compensate for evaporation in order to maintain a constant ionic concentration. At the conclusion of platinum-plated electrode testing, the procedure was repeated using ten iridium-plated stimulation sites.

Stimulation sites were photographed in color at 500 × magnification before and after the PBS stimulation tests. Before and after photographs were compared in order to spot any changes in insulation condition as well as stimulation site color and texture.

## III. Results

### A. Electrode Fabrication

The completed electrodes (Fig. 3) were flexible and durable enough to withstand repeated bending without breaking.

### B. In Vitro Testing

*1) Tip Shape:* Each of the initial insertion forces of the four blunt tips were averaged together to yield the average insertion force for blunt tips. The averaging was repeated for each subsequent insertion trial. The insertion forces for each of the other tip styles were also processed in this manner. The results are plotted in Fig. 4. According to a two-tailed, unequal variance $t$-test, each style was different from all of the others ($p < 0.001$).

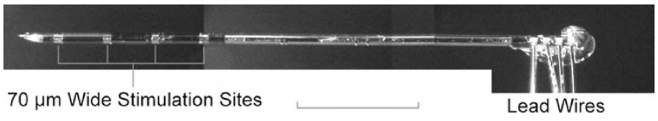


Fig. 3. Completed electrode (composite assembled from several micrographs). Lead wires are bonded to connection pads and are protected by epoxy. Insulated circuit traces run down the shaft linking each connection pad to one stimulation site. The tip was sharpened by a dicing saw. Calibration bar: 1 mm.

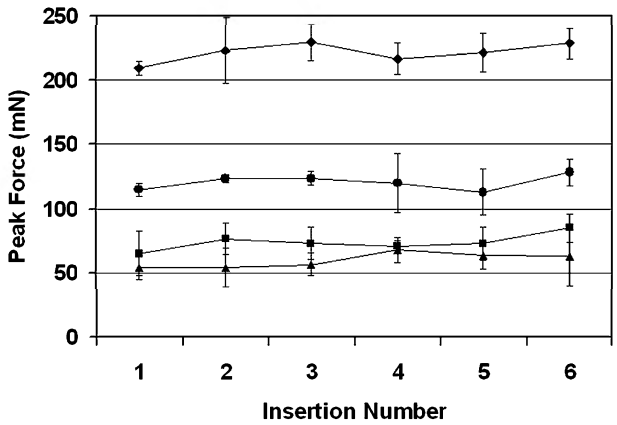


Fig. 4. Averaged peak insertion forces for each tip style: blunt (♦), chisel (●), hypo (■), and slant (▲). Each point represents the average of four different tips of similar tip shape. The error bars represent one standard deviation.

The blunt tip exhibited the highest and the slant tip the lowest average peak force.

No trend was observed in the forces required for penetration from the first insertion to the sixth insertion ($t$-test, $p > 0.1$) for any tip style. By comparing the before and after photographs of each fiber tip, no changes in tip shape, e.g., dulling or chipping, were observed.

*2) Insertion Effects on Impedance:* Insertion testing was performed on ten stimulation sites coated with platinum and ten sites coated with iridium. The interfacial impedance of platinum-coated electrodes increased from an average of 5.9 kΩ before insertions to 8.9 kΩ after insertions for an increase of $52 \pm 14\%$ (mean ± standard deviation). The interfacial impedance of iridium-coated electrodes increased from an average of 3.3 kΩ before insertions to 4.5 kΩ after insertions for a relative change of $36 \pm 23\%$. The initial impedances of the iridium sites were lower than those of the platinum sites ($t$-test, $p \ll 0.001$), but the relative changes in impedance were not statistically different ($t$-test, $p > 0.1$).

*3) Charge Delivery Capacity:* The impedance-change factor due to current passage was defined as the ratio of the average impedance measurement during the high-current testing to the average impedance measurements during the initial test sequence. Those stimulation sites which were given the 0.4 $\mathrm{mC/cm^2}$ test pulses had an average impedance-change factor of 0.90. Sites tested at 0.6 $\mathrm{mC/cm^2}$ showed an impedance-change factor of 1.0, 0.8 $\mathrm{mC/cm^2}$ resulted in a factor of 1.2, and 1.6 $\mathrm{mC/cm^2}$ generated a factor of 7.6. These values differ significantly (Kruskal–Wallis analysis of variance, $p < 0.05$). Fig. 5 illustrates the percentage of site failures, defined as impedance doubling, for each of the test currents. None of the site impedances in the 0.4 $\mathrm{mC/cm^2}$ or 0.6 $\mathrm{mC/cm^2}$ test

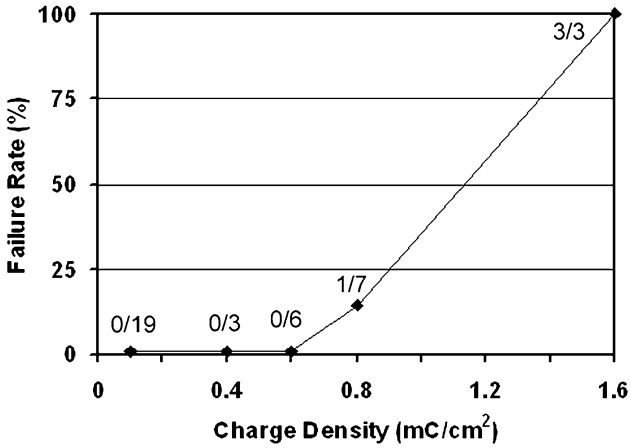


Fig. 5. Stimulation site response to high charge density pulse train testing. The fraction next to each point represents the number of electrodes that failed out of the number tested.

series doubled. One out of seven stimulation sites in the 0.8 $\mathrm{mC/cm^2}$ group more than doubled and all three of the sites that underwent 1.6 $\mathrm{mC/cm^2}$ more than doubled. Those sites which displayed large impedance changes also showed visible changes in the electrode surface.

Stimulation sites that exhibited small changes in impedance over the course of the stimulation schedule showed no visual change in the electrode surface. Sites which showed changes in impedance from 3 kΩ to 12–15 kΩ showed a mottled pattern of bluish black iridium metal interspersed with regions of gold metal. Electrodes which exhibited changes in impedance from 3 kΩ to over 100 kΩ, showed an absence of any metal on the substrate. There were no traces of metal flakes observed either on the electrodes or in the solution.

*4) Impedance Stability:* Data from the 12-day stimulation test of interfacial impedance were analyzed for three types of variation: measurement-to-measurement, diurnal, and overall trend. Measurement-to-measurement variations were observed and attributed to heater cycling of the hotplate. To confirm this observation, the hotplate was switched off. This eliminated the variations in impedance measurements for both the platinum- and iridium-plated stimulation sites. Diurnal variations corresponded to the two stimulation states: a 16-h stimulation period followed by an 8-h quiescent period. During quiescent periods, each platinum-plated electrode site showed a marked increase in impedance (Fig. 6) and these increases were proportional to the average impedance during stimulation ($t$-test, $p \ll 0.001$). In contrast, the impedances of the iridium-plated electrodes slightly decreased during quiescent periods (Fig. 7). The overall trend of the impedances of the platinum-plated sites was a 4.5% decrease from day 1 to day 12. The overall trend of the impedances of the iridium-plated sites was a 6.6% increase from the day 1 to day 12. In all cases, intratrace impedances remained above 1 MΩ.

Prior to the stimulation test, freshly plated films of iridium differed from platinum in color, texture, and coverage uniformity. Electroplated platinum was grey to black in color, appeared rough, and fully covered the underlying metal. Electroplated iridium appeared light blue to grey in color, showed little surface roughness, and contained distributed voids which had a

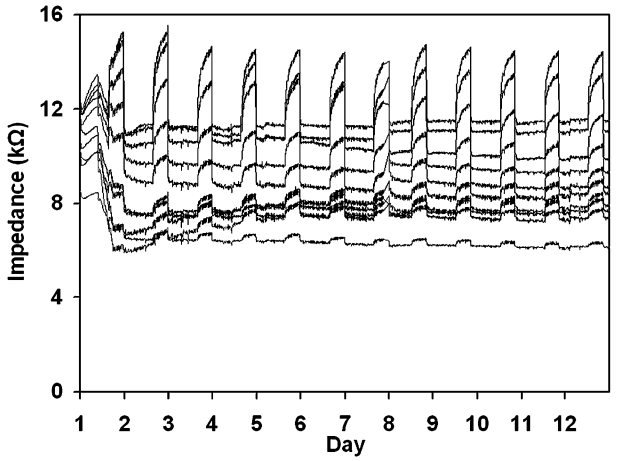


Fig. 6. Platinum-coated electrodes were submerged in heated PBS, were subjected to current pulses 16 h per day, and were measured 24 h per day. Each of the ten traces represents an individual stimulation site.

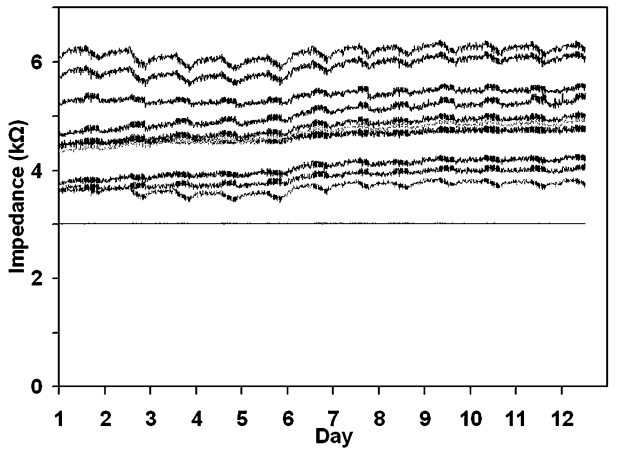


Fig. 7. Iridium-coated electrodes submerged in heated PBS were subjected to current pulses 16 h per day, and impedances were measured 24 h per day. Each of the ten traces represents an individual stimulation site. Additionally, measurement of an impedance standard with a value of 3 kΩ is shown to illustrate the stability of the measurement system.

gold color. Comparison of before and after micrographs showed no differences in either the electroplated metal or the insulation.

## IV. Discussion

### A. Fabrication

Although these electrodes were designed for chronic implantation in animal models, and their electrical and mechanical properties were tested, we did not experimentally evaluate their biocompatibility. The materials selected for the construction of the electrodes, except the polyimide insulation, are widely accepted to be biocompatible. Polyimide insulation on implanted electrodes has been shown to be biocompatible and durable [20]–[22], but the positive-tone photodefinable polyimide used here may contain ingredients that are not biocompatible. The negative-tone photodefinable polyimide (PI-2611, HD Microsystems) was reported as flexible but not fragile and "noncytotoxic according to ISO 10 993" [23], remaining intact up to 6 mo after implantation and inducing only mild fibrous reactions. [22]. While this material was a precursor to the polyimide we used here, HD-8000 should be formally tested for biocompatibility. Other proven biocompatible and bioresistant insulations, such as $SiO_2$ and parylene, are available but were not used due to processing difficulties.

### B. In Vitro Testing

*1) Tip Shape:* Since the peak insertion force for each tip remained constant throughout multiple insertions, we concluded that the tips remained sharp. This conclusion was supported by the comparison between before and after micrographs where no chipping or dulling was observed. Assuming that the simulated tissue used in these measurements adequately reflects the properties of spinal cord tissue, future cylindrical electrodes designed for tissue penetration should consider using the slant style tip as it had the lowest peak insertion force of those tested and was the easiest taper to produce.

*2) Insertion Effects on Impedance:* The electrodes were inserted more times than would be likely for intraspinal electrode placement. Electrode implant surgeries require each electrode be inserted into the spinal cord and then checked to determine if electrical stimulation results in the recruitment of the desired muscle group. If the recruitment is not as desired, the electrode needs to be removed and reinserted in a different position, sometimes requiring several insertions. The worst case observed during the insertion of 45 electrodes over a series of seven animal surgeries was an electrode that required four insertions into the spinal cord. By performing ten insertions with each electrode, the impedance increases observed during benchtop testing should represent the worst case scenario.

During the insertion test, iridium-plated electrodes displayed smaller impedance increases than platinum-plated electrodes. The more stable interface is an attractive feature of the iridium film. Additionally, the iridium-plated electrode impedances were 50% smaller than those of the platinum-plated electrodes. Lower impedances are beneficial because they can pass higher currents and still remain below the hydrogen evolution voltage. Therefore, iridium films are to be preferred over platinum films as the interfacial material for electrode sites.

*3) Charge Delivery Capacity:* The stimulation limit found for iridium-plated electrodes, between 0.60 and 1.6 $\mathrm{mC/cm^2}$, is consistent with the limit recommended by Beebe for cathodic-first pulses through activated iridium oxide film of 1.0 $\mathrm{mC/cm^2}$ [13]. Above this range the electrode metal will slowly be lost and the electrode will eventually fail. Stimulating with a charge density below 0.4 $\mathrm{mC/cm^2}$ should produce a metal dissolution rate well below 5 ng/C since it has been reported that charge densities below 0.4 $\mathrm{mC/cm^2}$ with current densities of 40 $\mathrm{mA/cm^2}$ in Pt produce dissolution rates less than that [19], and Ir has been shown to handle charge densities about an order of magnitude higher than Pt can [13].

There were no metal flakes visible on the sides of the electrodes or in the solution. This would suggest either the flakes were too small to observe or that the metal was not lost through delamination but rather through dissolving into solution during high current cathodal stimulation. Metal loss by dissolution is consistent with the results found by Brummer which indicated

excessive stimulation of platinum electrodes caused the platinum to dissolve into inorganic saline solution [19].

*4) Impedance Stability:* All 20 stimulation sites used in the impedance stability test displayed stable and consistent behavior. Three symptoms of electrode failure were monitored: steady decreases in impedance, steady increases in impedance, and sharp, drastic increases in impedance. Any sustained decreases in impedance would have indicated a delamination of insulation, but this was not observed. Small sustained increases in impedance would have indicated a possible loss of interfacial metal into solution. This too was not seen. Finally, any impedances rapidly rising to megaohm levels could indicate a bond failure or a break in a circuit trace. Although this kind of impedance spike was observed during pilot studies, improvements in the bonding method eliminated open-circuit failures. The spontaneous loss of iridium oxide activation reported by Loeb was not observed during our testing [24]. It appears that the cylindrical electrode sites are capable of passing charge through many cycles without sustaining noticeable damage.

### C. Other Uses

Although the cylindrical electrodes were designed with stimulation in mind, these electrodes have the potential to record neural activity. In a pilot study, electrically evoked compound action potentials were recorded in the ventral horn of the spinal cord. The capability to provide both recording and stimulating sites on the same electrode shaft merits further investigation.

The electrodes described here have also been built, as prototypes only, on fluid-conducting capillary tubing and optically active fibers. This capability could lead to new opportunities. Building electrodes on capillary tubing may permit researchers to stimulate or record neurons while the electrode core injects fluids such as drugs, saline, or glucose. The insertion site could also be flushed or aspirated to remove either enzymes or foreign body response factors from the penetration site.

The fabrication of electrodes around optical fibers also offers opportunities. After inserting the electrode/fiber optic into neural tissue, the tissue can be stimulated or recorded from either electrically or optically. One use of the optical capacity could be for the treatment of brain tumors by photodynamic therapy. The electrode could be used to record neural activity and, therefore, determine the position within the laminae, then light could be delivered to the photosensitized tumor. Photoactivation of porphyrin by 630 nm light has been shown to destroy malignant tissue [25]. Our prototypes have successfully demonstrated the ability to transmit 632 nm light through the center of the electrode. In addition to sending light into tissue, light emitted from tissue (e.g., by luminescence compounds) could be collected and processed to yield spectral data.

### D. Further Improvements

The cylindrical electrodes described here may need to be improved for better acceptance in the body. In a review on the future of intraspinal stimulation, the preferred diameter of cylindrical electrodes was stated as smaller than 50 $\mu$m [26]. Recent improvements in cylindrical microfabrication equipment may offer the ability to produce electrodes on 65-$\mu$m-diameter fibers, but this size reduction would come at the cost of electrode site area and, therefore, charge delivery capacity.

Another potential improvement in cylindrical electrodes is a reduction in bond junction size. When the electrode is implanted within the spinal cord, the bond junction sticks out above the spinal cord. In chronic applications, this creates a condition where overlying tissue could rub against the electrode, potentially dislodging or relocating it [27]. In order to minimize this hazard, the length of the bond junction protruding above the spinal cord must be reduced, which may require considering a different electrode/lead wire configuration.

In conclusion, the existing design appears suitable for acute testing in animal preparations, as demonstrated in the companion paper [28]. Modification of the junction between the electrode and connecting wires, and a possible slight reduction in electrode diameter, should produce a system suitable for use in chronic animal studies.

## ACKNOWLEDGMENT

The authors thank Dr. D. Normann for advice on sources of measurement variation during long-term impedance testing and both Dr. A. Prochazka and Dr. V. Mushahwar for advice on electrode design.

## REFERENCES

[1] M. Sharma, E. B. Marsolais, G. Polando, R. J. Triolo, J. A. J. Davis, N. Bhadra, and J. P. Uhlir, "Implantation of a 16-channel functional electrical stimulation walking system," *Clin. Orthop.*, vol. 347, pp. 236–242, 1998.

[2] Z. Fang and J. T. Mortimer, "Selective activation of small motor axons by quasitrapezoidal current pulses," *IEEE Trans. Biomed. Eng.*, vol. 38, no. 2, pp. 168–174, Feb. 1991.

[3] R. L. Waters, D. McNeal, and J. Perry, "Experimental correction of footdrop by electrical stimulation of the peroneal nerve," *J. Bone Joint Surg.*, vol. 57A, pp. 1047–1054, 1975.

[4] V. K. Mushahwar, D. F. Collins, and A. Prochazka, "Spinal cord microstimulation generates functional limb movements in chronically implanted cats," *Exp. Neurol.*, vol. 163, pp. 422–429, 2000.

[5] K. Najafi, J. Ji, and K. D. Wise, "Scaling limitations of silicon multichannel recording probes," *IEEE Trans. Biomed. Eng.*, vol. 37, no. 1, pp. 1–11, Jan. 1990.

[6] P. S. Motta and J. W. Judy, "Multielectrode microprobes for deep-brain stimulation fabricated using a novel 3-d shaping electroplating process," presented at the Digital Solid-State Sensor and Actuator Workshop, Hilton Head Island, SC, 2002.

[7] P. Pochay, K. D. Wise, L. F. Allard, and L. T. Rutledge, "A multichannel depth probe fabricated using electron-beam lithography," *IEEE Trans. Biomed. Eng.*, vol. BME-26, pp. 199–206, 1979.

[8] M. Esashi, K. Minami, and S. Shoji, "Optical exposure systems for three-dimensional fabrication of microprobe," in *Proc. IEEE Microelectromechanical Systems*, Hara, Japan, 1991, pp. 39–44.

[9] V. K. Mushahwar and K. W. Horch, "Proposed specifications for a lumbar spinal cord electrode array for control of lower extremities in paraplegia," *IEEE Trans. Rehabil. Eng.*, vol. 5, no. 3, pp. 237–243, Sep. 1997.

[10] S. C. Jacobsen, D. L. Wells, C. C. Davis, and J. E. Wood, "Fabrication of micro-structures using nonplanar lithography (NPL)," presented at the IEEE Micro Electro Mechanical Systems, Nara, Japan, 1991.

[11] D. L. Wells, "Non-planar microfabrication," Univ. Utah, Dept. Bioeng., Salt Lake City, UT, 1993.

[12] S. B. Brummer, L. S. Robblee, and F. T. Hambrecht, "Criteria for selecting electrodes for electrical stimulation: Theoretical and practical considerations," *Ann. New York Acad. Sci.*, vol. 405, pp. 159–171, 1983.

[13] X. Beebe and T. L. Rose. "Charge injection limits of activated iridium oxide electrodes with 0.2 ms pulses in bicarbonate buffered saline." *IEEE Trans. Biomed. Eng.*, vol. 35, no. 6, pp. 494–495, Jun. 1988.
[14] V. K. Mushahwar and K. W. Horch. "Muscle recruitment through electrical stimulation of the lumbo-sacral spinal cord." *IEEE Trans. Rehabil. Eng.*, vol. 8, no. 1, pp. 22–29, Mar. 2000.
[15] M. R. McNeely. "Development and validation of micro structure fabrication using cylindrical lithography." Univ. Utah, Dept. Bioeng., Salt Lake City, 1997.
[16] K. R. Cote and R. C. Gill. "Development of a platinized platinum/iridium electrode for use in vitro." *Ann. Biomed. Eng.*, vol. 15, pp. 419–426, 1987.
[17] T. G. McNaughton and K. W. Horch. "Metallized polymer fibers as leadwires and intrafascicular microelectrodes." *J. Neurosci. Meth.*, vol. 70, pp. 103–110, 1996.
[18] D. J. Edell, V. V. Toi, V. M. McNeil, and L. D. Clark. "Factors influencing the biocompatibility of insertable silicon microshafts in cerebral cortex." *IEEE Trans. Biomed. Eng.*, vol. 39, no. 6, pp. 635–643, Jun. 1992.
[19] S. B. Brummer, J. McHardy, and M. J. Turner. "Electrical stimulation with Pt electrodes: Trace analysis for dissolved platinum and other dissolved electrochemical products." *Brain, Behavior, Evol.*, vol. 14, pp. 10–22, 1977.
[20] H. S. Haggerty and H. S. Lusted. "Histological reaction to polyimide films in the cochlea." *Acta Oto-Laryngologica*, vol. 107, pp. 13–22, 1989.
[21] L. A. Geddes and R. Roeder. "Criteria for the selection of materials for implanted electrodes," *Ann. Biomed. Eng.*, vol. 31, pp. 879–890, 2003.
[22] F. J. Rodríguez, D. Ceballos, M. Schuttler, A. Valero, E. Valderrama, T. Stieglitz, and X. Navarro. "Polyimide cuff electrodes for peripheral nerve stimulation." *J. Neurosci. Meth.*, vol. 98, pp. 105–18, 2000.
[23] A. Schneider and T. Stieglitz. "Implantable flexible electrodes for functional electical stimulation." *Med. Device Technol.*, vol. 15, pp. 16–18, 2004.
[24] G. E. Loeb, R. A. Peck, and J. Martyniuk. "Toward the ultimate metal microelectrode," *J. Neurosci. Meth.*, vol. 63, pp. 175–183, 1995.
[25] P. J. Muller and B. C. Wilson. "Photodynamic therapy of malignant brain tumors." *Can. J. Neurolog. Sci.*, vol. 17, pp. 193–198, 1990.
[26] A. Prochazka, V. K. Mushahwar, and D. McCreery. "Neural prostheses." *J. Physiol.*, vol. 533, pp. 99–109, 2001.
[27] B. J. Woodford, R. R. Carter, D. McCreery, L. A. Bullara, and W. F. Agnew. "Histopathologic and physiologic effects of chronic implantation of microelectrodes in sacral spinal cord of the cat." *J. Neuropathol. Exp. Neurol.*, vol. 55, pp. 982–991, 1996.
[28] S. Snow, K. W. Horch, and V. K. Mushahwar. "Intraspinal microstimulation using cylindrical multielectrodes." *IEEE Trans. Biomed. Eng.*, vol. 53, no. 3, pp. 311–319, Feb. 2005.

**Sean Snow** (S'02–M'05) received the B.E.E. degree in electrical engineering from Georgia Institute of Technology, Atlanta, in 1992 and the Ph.D. degree in bioengineering from the University of Utah, Salt Lake City, in 2005.

He served in the U.S. Peace Corps from 1992 to 1994 teaching physics in the Fiji Islands. He worked from 1995 to 1998 at Nikon Precision Inc., Belmont, CA, installing step-and-repeat systems for industrial photolithography applications.

Dr. Snow was awarded the Whitaker Foundation Graduate Fellowship from 1999 to 2004.

**Stephen C. Jacobsen** (M'91), received the B.S. and M.S. degrees in mechanical engineering from the University of Utah, Salt Lake City, in 1967 and 1968, and received the Ph.D. degree in mechanical engineering from the Massachusetts Institute of Technology, Boston, in 1973.

He is a Distinguished Professor of Mechanical Engineering at the University of Utah. He founded Sarcos Research Corporation (SRC) to augment development activities at the university and is the Chairman and CEO of Sarcos in Salt Lake City.

**David L. Wells** received the B.S. degree in electrical engineering from the University of Arizona, Tucson, in 1986. He received the M.S. and Ph.D. degrees in bioengineering from the University of Utah, Salt Lake City, in 1989 and 1993, respectively.

He is currently Electronics Coordinator in the Rehabilitation Engineering Department at the Bloorview MacMillan Children's Centre in Toronto, ON, Canada, and Adjunct Assistant Professor in the Institute of Biomaterials and Biomedical Engineering at the University of Toronto.

**Kenneth W. Horch** (M'88) received the B.S. degree from Lehigh University, Bethlehem, PA, and the Ph.D. degree from Yale University, New Haven, CT.

He is currently Professor of Bioengineering and Professor of Physiology at the University of Utah, Salt Lake City.

Dr. Horch is an AIMBE Fellow. For more information visit http://www.bioen.utah.edu/faculty/KWH.